SANDIA REPORT
SAND2012-1292
Unlimited Release
March 2012

Surface Photovoltage Measurements and Finite Element Modeling of SAW Devices

Christine Donnelly

Prepared by
Sandia National Laboratories
Albuquerque, New Mexico 87185 and Livermore, California 94550

Sandia National Laboratories is a multi-program laboratory managed and operated by Sandia Corporation, a wholly owned subsidiary of Lockheed Martin Corporation, for the U.S. Department of Energy's National Nuclear Security Administration under contract DE-AC04-94AL85000.

Issued by Sandia National Laboratories, operated for the United States Department of Energy by Sandia Corporation.

Available to DOE and DOE contractors from
U.S. Department of Energy
Office of Scientific and Technical Information
P.O. Box 62
Oak Ridge, TN 37831

Telephone: (865) 576-8401
Facsimile: (865) 576-5728
E-Mail: reports@adonis.osti.gov
Online ordering: http://www.osti.gov/bridge

Available to the public from
U.S. Department of Commerce
National Technical Information Service
5285 Port Royal Rd.
Springfield, VA 22161

Telephone: (800) 553-6847
Facsimile: (703) 605-6900
E-Mail: orders@ntis.fedworld.gov
Online order: http://www.ntis.gov/help/ordermethods.asp?loc=7-4-0#online

SAND2012-1292
Unlimited Release
March 2012

Surface Photovoltage Measurements and Finite Element Modeling of SAW Devices

Christine Donnelly
1749
Sandia National Laboratories
P.O. Box 5800
Albuquerque, New Mexico 87185-MS1080

Abstract

Over the course of a Summer 2011 internship with the MEMS department of Sandia National Laboratories, work was completed on two major projects. The first and main project of the summer involved taking surface photovoltage measurements for silicon samples, and using these measurements to determine surface recombination velocities and minority carrier diffusion lengths of the materials. The SPV method was used to fill gaps in the knowledge of material parameters that had not been determined successfully by other characterization methods.

The second project involved creating a 2D finite element model of a surface acoustic wave device. A basic form of the model with the expected impedance response curve was completed, and the model is ready to be further developed for analysis of MEMS photonic resonator devices.

Table of Contents

Section 1: Surface Photovoltage Measurements

Introduction

The surface photovoltage (SPV) technique is a contactless method for measuring properties of semiconductor wafers without causing damage to the samples. It is often used to measure the quality of samples, and to determine material parameters. The technique consists of shining monochromatic light on a sample wafer, and measuring the resulting change in surface potential with a lock-in amplifier.

The SPV measurement technique was used to determine surface recombination velocities and minority carrier diffusion lengths of silicon samples that were fabricated using a variety of passivation methods. This data was used to supplement measurements taken using the photoconductance decay method.

Background:

Theory:

At the surface of a semiconductor material, dangling bonds create energy states that do not exist in the bulk material. These states serve as a trap for charge carriers, and cause there to be a net positive charge at the surface if the semiconductor is a p-type material. This nonzero charge distribution causes an electric field to exist at the material's surface, which sweeps free charge carriers out of a region near the surface known as the space-charge region.

When the material is illuminated by photons that are above the bandgap energy, electron-hole pairs are created and additional carriers will be swept either away from or toward the surface, causing the surface voltage to change. For p-type semiconductors, electrons are brought to the surface and holes move away from the surface. The change in surface voltage is measured in the SPV process. Only those generated charge carriers that reach the space-charge region before recombining with a charge carrier of the opposite type will contribute to a change in the surface voltage. Therefore, the measurement provides a means of determining the distance that charge carriers diffuse through the material before recombining: the minority carrier diffusion length.

The minority carrier diffusion length is an important parameter for devices such as solar cells that rely on diffusion of charge carriers across a depletion region. In addition, the diffusion length can be used to measure defect densities in semiconductor materials. The minority carrier diffusion length can be expected to decrease when defect densities increase.

Surface recombination velocity is an additional important parameter for prediction of device performance. For devices such as solar cells, a high SRV is undesirable because this means that charge carriers are moving to the surface of the material and not contributing to current through the load.

The analysis of the surface photovoltage begins with the continuity equation for a semiconductor in stready-state:

$$D\frac{d^2\delta n(x)}{dx^2} - \frac{\delta n(x)}{\tau} + G(x) = 0$$

where D is the diffusion coefficient, G is the generation and τ is the minority carrier lifetime.

At the top surface of the material, a boundary condition for this equation is:

$$\left.\frac{d\delta n(x)}{dx}\right|_{x=0} = s_1\frac{\delta n(x=0)}{D}$$

Where s1 has units of velocity and is known as the surface recombination velocity.

At the bottom surface of the material, the boundary condition can be written:

$$\left.\frac{d\delta n(x)}{dx}\right|_{x=W} = -s_2\frac{\delta n(x=d)}{D}$$

Finally, when there is light incident on the sample, the generation is given by

$G(x,\lambda) = I_o(\lambda)\alpha(\lambda)(1-R)*\exp(-\alpha x)$,

where R is the reflectivity, α is the wavelength-dependent absorption coefficient and I_o is the incident photon flux (photon/(sec•cm^2)).

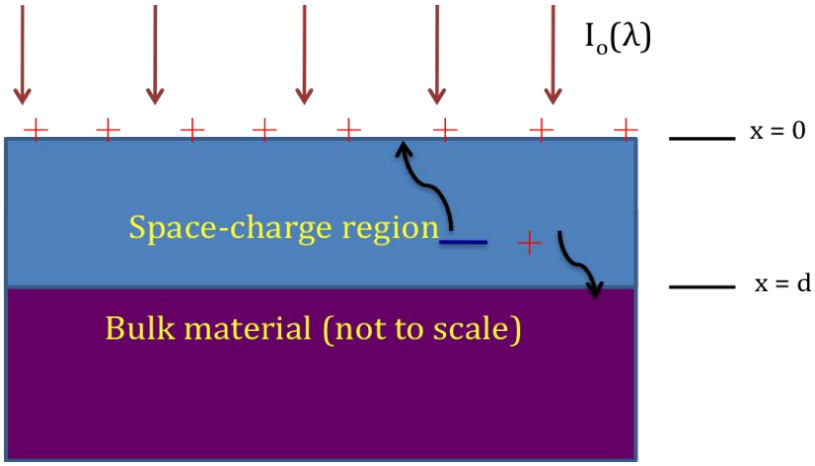

Figure 1: Illuminated P-type wafer

The solution to the continuity equation, given these boundary conditions, is a complex expression with hyperbolic sine and cosine terms. However, the result can be simplified substantially when the following assumptions are made:

1) Space-charge region width is much smaller than wafer thickness.
2) Wafer is much thicker than minority carrier diffusion length
3) Back contact has high surface recombination, so that s2 becomes infinitely large.

After making these assumptions, the equation for excess carrier concentration at the space-charge region boundary becomes:

$$\delta n(W) = \frac{(1-R)I_o}{(s1+\frac{D}{L_n})} * \frac{L_n}{(L_n+\frac{1}{\alpha})}$$

Assuming that the surface photovoltage is directly proportional to the excess carrier concentration at the edge of the space-charge region, $\delta n(W) = \frac{n_i e V}{kT}$ (the "Law of Junction" for eV>>kT), the equation can be rewritten:

$$\frac{1}{V} = \left(\frac{n_i e}{kT}\right) \frac{\left(\frac{D}{L_n} s1\right)}{I_o(1-R)L_n} \left[\frac{1}{\alpha} + L_n\right]$$

When the equation is written in this form, it is apparent that plotting (1/V) vs. (1/α), both of which are wavelength-dependent properties, will yield a line with an x-intercept of $-L_n$. A graph in this form is known as a Goodman Plot.

Applications:

The main experimental objective was to characterize a variety of silicon samples intended for solar cell applications. These samples were created using a range of fabrication and surface passivation methods. The samples included both Czochralski and float zone wafers that either had no oxide layer, or a 20 nm layer produced by either the wet or dry deposition method. Some of the samples also had a 60 nm nitride layer deposited either by plasma enhanced chemical vapor deposition (PECVD) or low pressure chemical vapor deposition (LPCVD). PECVD, which tends to cause surface passivation by creating a positively charged layer at the surface of the sample, is currently the preferred passivation method for solar cells. The LPCVD method mainly causes surface passivation by filling dangling bonds and is not generally used for solar cell applications. However, LPCVD has the advantage that it can be used to fully coat all surfaces of a sample with nitride, rather than only the top exposed surface.

Because the samples were intended for an application that requires LPCVD coating, one goal of the measurements was to determine whether samples that used the LPCVD nitride deposition process could achieve reasonably low surface recombination velocities and high minority carrier diffusion lengths. The more general goal was to determine optimal surface passivation methods for solar cells.

Materials and Methods

Experimental Setup:

A monochromator containing a diffraction grating was used to filter input light from a lamp, and produce output light over a narrow wavelength range. The light source was chopped at approximately 150 Hz using an optical chopper, and light traveled via a fiber-optic cable to the sample. The sample was illuminated and the resulting change in surface voltage was measured with a lock-in amplifier using capacitive coupling techniques.

Through LabView interfacing with the monochromator and lock-in amplifier, a wavelength sweep was taken and the resulting change in voltage was measured at each wavelength. The measurement time constant was one second, and 3 measurements were averaged per wavelength step.

Measurement Techniques:

Narrowing light bandwidth:

While the monochromator would ideally produce light at a single wavelength, in reality the light output contains a range of wavelengths. The light from a lamp is separated by the instrument's diffraction grating, and the angle of an internal mirror determines which of the diffracted wavelengths leave through the instrument's output slit. Therefore, the wider the slit width, the larger the output bandwidth. A variety of slit widths were tried in order to find a balance between eliminating light noise and obtaining a detectable signal. The bandwidth was eventually reduced to under 20 nm with a 30 micrometer slit width. At lower slit widths, the intensity of incident light on the sample was too low to yield a measureable change in surface voltage.

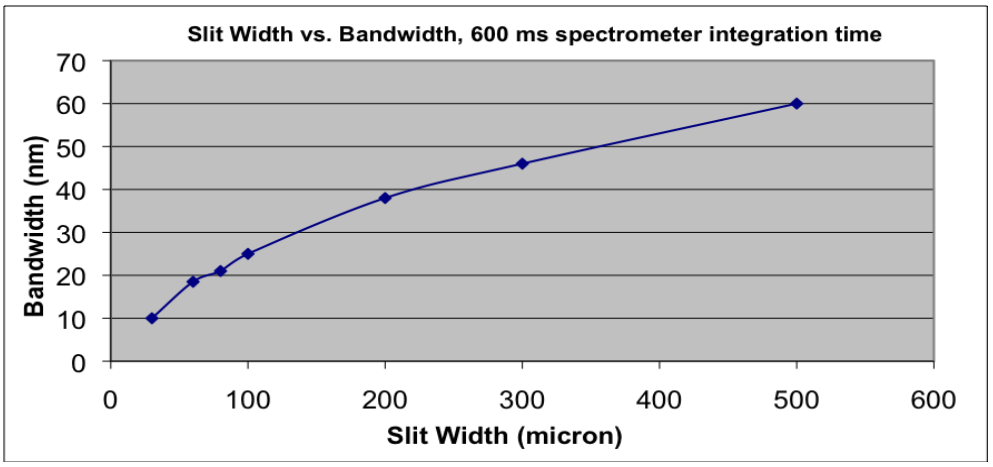

Figure 2: Light Bandwidth vs. Monochromator Slit Width

Monochromator calibration:

A thorough calibration of the monochromator was performed. Because the absorption coefficient is highly wavelength-dependent in the range of wavelengths being used, even small calibration errors are undesirable.

Multiple steps were taken to ensure accurate calibration. A ThorLabs spectrometer measured light output from four different spectral calibration lamps (Hg, Xe, Ar, and Kr). By comparing multiple spectral lines that occur at known wavelengths with the measured spectrometer value, the spectrometer calibration offset was determined. The spectrometer could then be accurately used to test the monochromator output wavelength, and to recalibrate the monochromator.

The calibration accuracy was independently double-checked by using light filters for which there exist published intensity-vs.-wavelength curves. Intensity sweeps were taken with the monochromator while a filter was in place, and the measured intensity-wavelength curves were compared to the published plots.

Photon flux normalization:

The photon flux must be known in order to use Goodman plots and accurately calculate the minority carrier diffusion length of the samples. To determine photon flux, the fiber-optic cable output was measured with a photodetector immediately following each SPV measurement sweep. The photodetector current and its known responsivity-vs.-wavelength curve (amps/watt) was used to determine power, as well as photon flux.

Surface reflectivity:

The surface reflectivity was measured using a spectrophotometer. Light was shined onto the sample with a monochromator, and the amount of reflected vs. absorbed light was measured. Reflectivity data for the seven silicon samples measured is shown in Appendix A.

Results:

An SPV signal could be detected for seven of the silicon samples. The Goodman Plot for these samples is shown in Figure 3. The samples that were coated with a nitride layer using the PECVD deposition technique did not produce a measureable SPV signal, due to the fact that their minority carrier diffusion lengths were greater than the sample thickness (650 um), which violates one of the assumptions used when relating surface photovoltage to minority carrier diffusion length.

Values for minority carrier diffusion length and lifetime, as well as surface recombination velocities, are shown in table format in Appendix A.

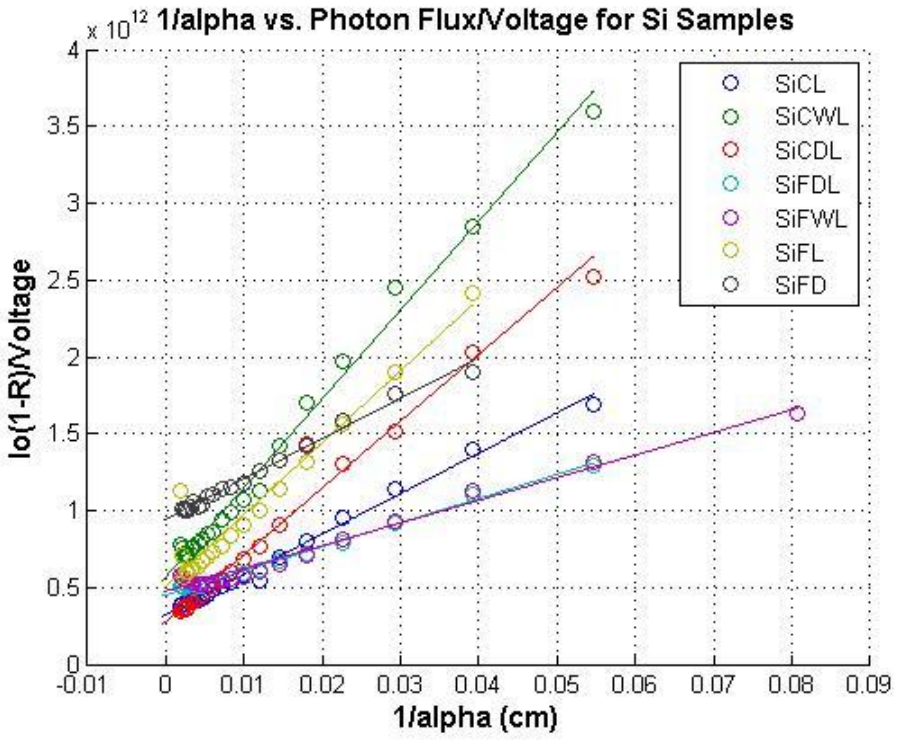

Figure 3: Goodman Plot for silicon samples

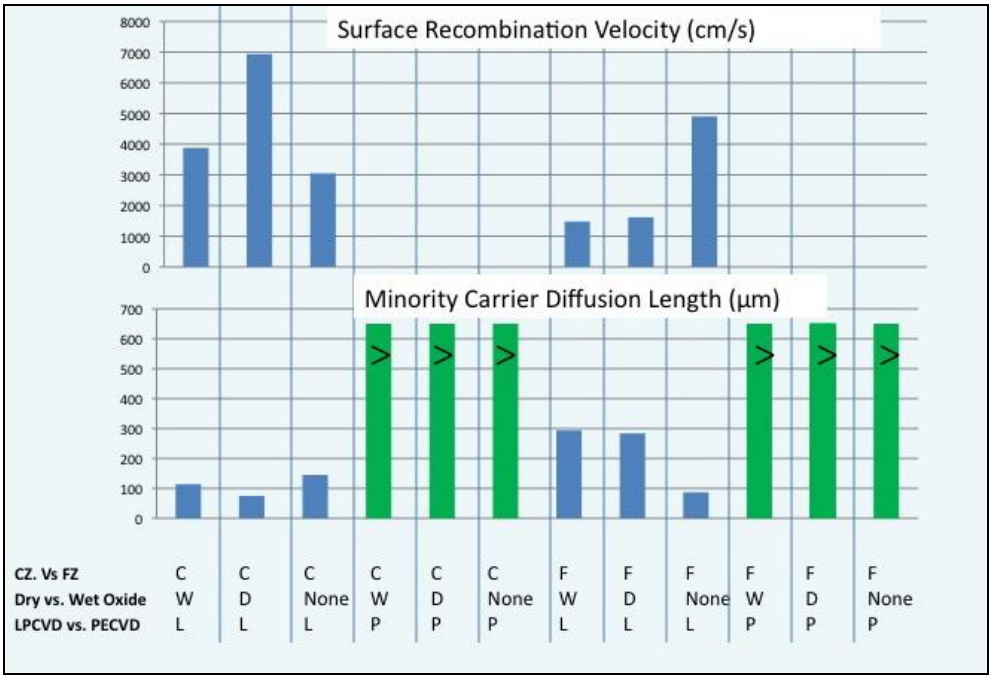

Figure 4: Surface recombination velocities and minority carrier diffusion lengths for silicon samples

Discussion and Future Steps:

Using the surface photovoltage technique, multiple samples that could not be measured using the photoconductance decay method due to their relatively low diffusion lengths were able to be characterized. An additional variable which must be explored before passivation techniques can be directly compared is the contamination levels of the equipment in the fabrication facilities. Samples that have been fabricated using equipment with higher contamination levels will see a decrease in minority carrier diffusion length that is not due solely to the intrinsic quality of the passivation method. Therefore, the results can only be used to compare the efficacy of passivation techniques that take place using the Sandia fabrication facilities, and cannot yet be extended to make general conclusions about optimal surface passivation methods.

In order to separate the effectiveness of a passivation method from the contamination levels of equipment, an additional set of experiments must be performed in which minority carrier diffusion lengths are measured before and after the use of fab equipment for each individual process. In order to take these measurements, the amount of noise contamination in the experimental setup must be decreased so that a signal can be measured for bare silicon samples, which will have higher recombination velocities, low diffusion lengths and low overall changes in surface voltage with photonic excitement.

Sect 2: COMSOL Modeling of Surface Acoustic Wave Resonators

Background and Motivation:

The purpose of this project was to produce a basic 2-D finite element model of a surface acoustic wave (SAW) device, and then to expand this model to account for varying device geometries and materials. The FEM model will eventually be used to analyze MEMS photonic resonator devices that function similarly to SAW devices and are being developed at Sandia .

SAWs are waves that are generated at the free surface of an elastic solid. In a typical two-port surface acoustic wave device, there are two IDTs (interdigital transducers) which consist of metal fingers deposited on a piezoelectric material that are connected to either a ground or signal busbar. One of the IDTs serves to convert an alternating voltage on the busbars into mechanical waves in the piezoelectric material. Reflectors that surround the IDTs consist of grounded metal fingers with the same spacing as the IDT fingers, and these serve to trap acoustic energy within the device. The other IDT then converts the vibrations into an output signal. A two-port resonator device is shown in Figure 5.

SAW and photonic resonator devices can act as filters and have applications for a variety of technologies, such as cell phones. The metal fingers for the IDTs are spaced at some design resonance frequency. When the input signal is at the resonance frequency, standing waves will be produced in the IDT region and the device will have low impedance, producing a high output current. At other frequencies, this phenomenon will not occur, and the current response of the device will be low.

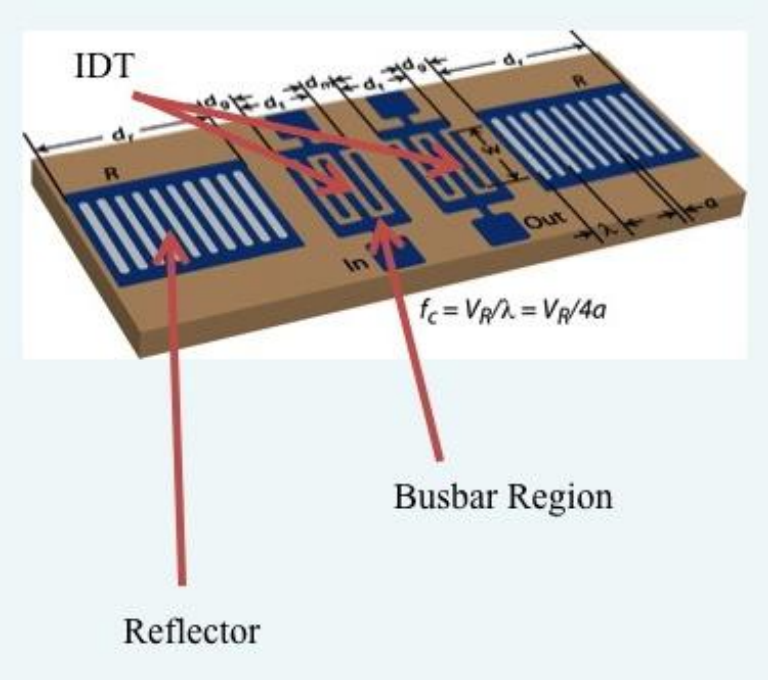

Figure 5: Typical two-port resonator SAW device

Although a number of one-dimensional models of surface acoustic wave devices currently exist, the goal was to create an accurate model that captures two-dimensional effects. With a one-dimensional model, the impact of all regions of the device cannot be accurately modeled. For example, the equations governing wave propagation through the devices might be solved along a line that runs through the reflectors and IDT, but effects of the busbars would be ignored.

A main question that the 2D model can answer is how much wave energy leaks through the busbars, versus how much remains trapped in the device. One effect of unexpected reflections and/or leakage at the busbars is to alter the impedance response of SAW devices. Ideally the impedance curves would be smooth with a resonance peak, but busbar effects can cause small oscillations in the response known as spurious modes. Through 2D modeling, the effects of device geometry alterations on the impedance curves and spurious modes can be explored.

One method commonly used to analyze wave propagation in SAW devices is the Coupling of Modes technique. A general idea of the derivation of the one-dimensional COM equations is described below:

Initially, a wave is written as a field φ(x). Using the loaded wave equation, the field can be written

$$\left(\frac{d}{dx^2} + {k_0}^2\right)\varphi(x) = -\sigma(x){k_0}^2\varphi(x)$$

The field can also be written as φ(x)=exp(-iβx)*Φ(x), where Φ(x) is periodic with period p and β is a wavenumber. By design, the spacing of the IDT fingers will be such that they have a half-period s, corresponding to a total period of 2s and a wavenumber β_{IDT} = (pi/s). This characteristic wavenumber which is meant to match the resonance wavenumber of excitations to the device. Therefore, at design conditions, β_{input} = n*pi/s. Using the COM technique, the input wavenumber is assumed to be β_{input} = n*pi/s + q, where q is a small deviation from the resonance wavenumber.

Because Φ(x) is periodic with period p, it has a Fourier series and can be written in terms of a sum of harmonic wavenumbers,

$$\frac{2\pi n}{p}$$

The field φ(x) can therefore also be written in terms of a sum of complex exponentials with wavenumbers $\beta_n = \beta + \frac{2\pi n}{p}$, or in the case of input waves for a SAW device near resonance frequency, $\beta_n = q + \frac{\pi n}{s}$. Taking only the harmonics n=1 and n=-1, the total expression then becomes $\varphi(x) = \varphi_1 e^{(-iqx)} e^{(\frac{i\pi x}{s})} + \varphi_{-1} e^{(-iqx)} e^{(\frac{i\pi x}{s})}$.

If the terms are substituted into the loaded wave equation, under a number of simplifying assumptions, terms can be recombined to form the following set of equations for the IDT region of the device:

$$\frac{dA^+(x)}{dx} = -i\delta A^+ + ikA^-(x)$$

$$\frac{dA^-(x)}{dx} = -ik^* A^- + i\delta A^-(x)$$

Using a two-dimensional loaded wave equation and adding in a periodic voltage forcing with amplitude V, the equations describing the movement of waves through a SAW device become:

$$\frac{\partial A^-(x)}{\partial x} = -i\delta A^+(x) - ik_{12}A^-(x) - j\frac{\gamma}{2k_0}\frac{\partial^2 A^-(x)}{\partial y^2} + \alpha V$$

$$\frac{\partial A^-(x)}{\partial x} = -ik_{12}^{*}A^+(x) + i\delta A^-(x) - j\frac{\gamma}{2k_0}\frac{\partial^2 A^-(x)}{\partial y^2} + \alpha V$$

In the reflector region of the device, where there are fingers at half-period spacing s but no applied voltage, the equations become:

$$\frac{\partial A^-(x)}{\partial x} = -i\delta A^+(x) - ik_{12}A^-(x) - j\frac{\gamma}{2k_0}\frac{\partial^2 A^-(x)}{\partial y^2}$$

$$\frac{\partial A^-(x)}{\partial x} = -ik_{12}^{*}A^+(x) + i\delta A^-(x) - j\frac{\gamma}{2k_0}\frac{\partial^2 A^-(x)}{\partial y^2}$$

In the busbar region of the device, where no fingers exist and there are no internal reflections, the equations become:

$$\frac{\partial A^-(x)}{\partial x} = -i\delta A^+(x) - j\frac{\gamma}{2k_0}\frac{\partial^2 A^+(x)}{\partial y^2}$$

$$\frac{\partial A^-(x)}{\partial x} = i\delta A^-(x) - j\frac{\gamma}{2k_0}\frac{\partial^2 A^-(x)}{\partial y^2}$$

Initial Modeling

One-Dimensional Model

A model of the SAW devices was created using COMSOL, a finite element modeling program. The one-dimensional COM equations were initially solved to ensure modeling accuracy. Results of this model, which displayed the expected resonance behavior, are shown in Figure 6.

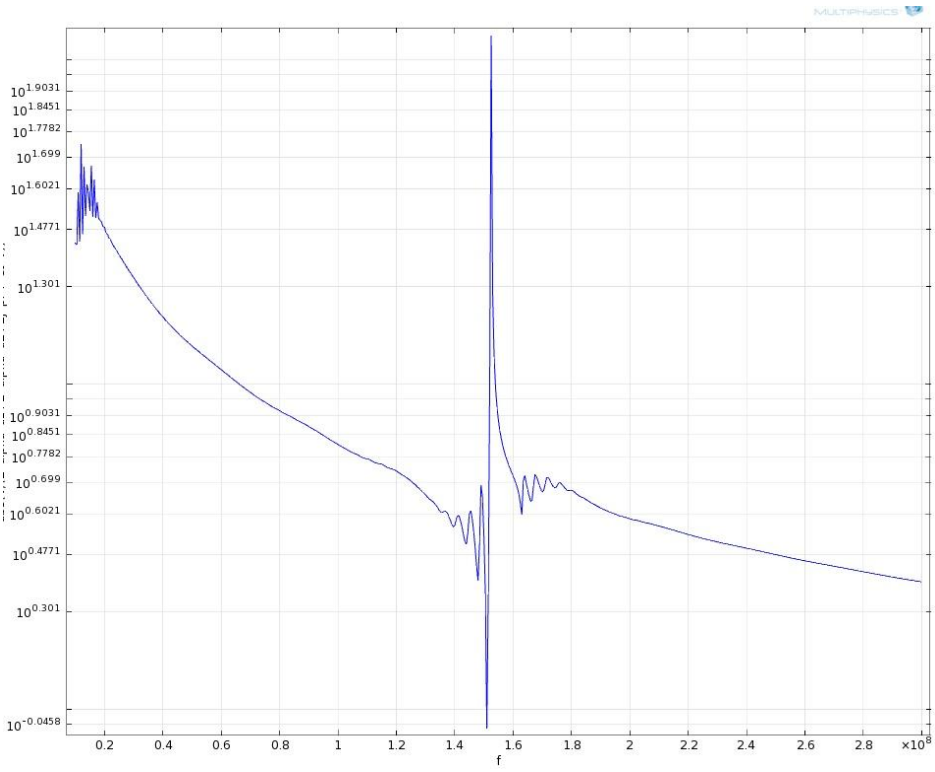

Figure 6: Impedance vs. frequency for 1D COMSOL model

Two-Dimensional Model

For the two-dimensional model, separate equations were assigned to each region of the device and continuity boundary conditions were applied. A PML (perfectly matched layer) was also added to the model to account for the gradual decay of wave amplitude outside the boundaries of the device. The 2D model used is shown in figure 7.

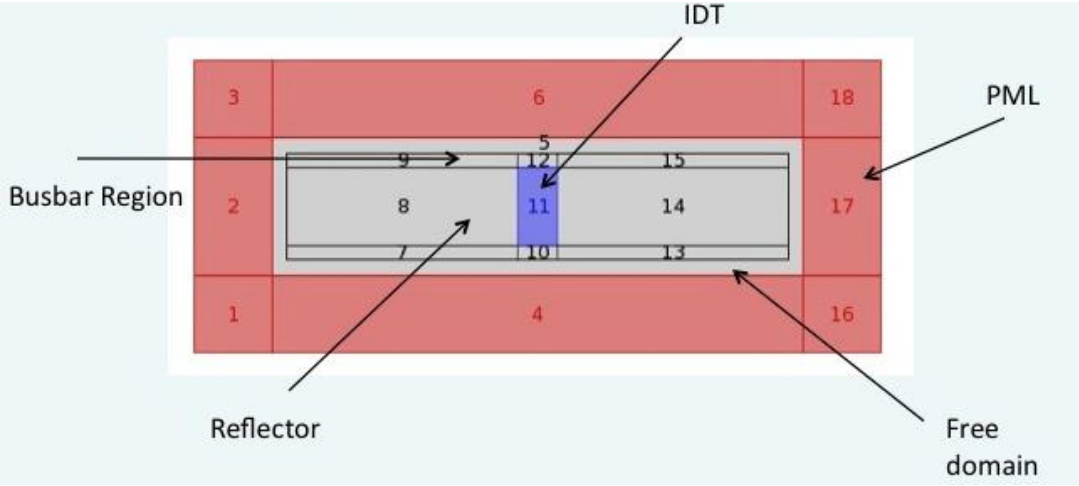

Figure 7: COMSOL model of one-port SAW device

Results are shown in figures 8 and 9. Although a more fine frequency sweep would be required to recreate a smooth impedance response curve, the expected resonance behavior can be seen. The spatial solution (shown at the design resonance frequency) displays the expected standing wave behavior and rapid amplitude decay in the PML region.

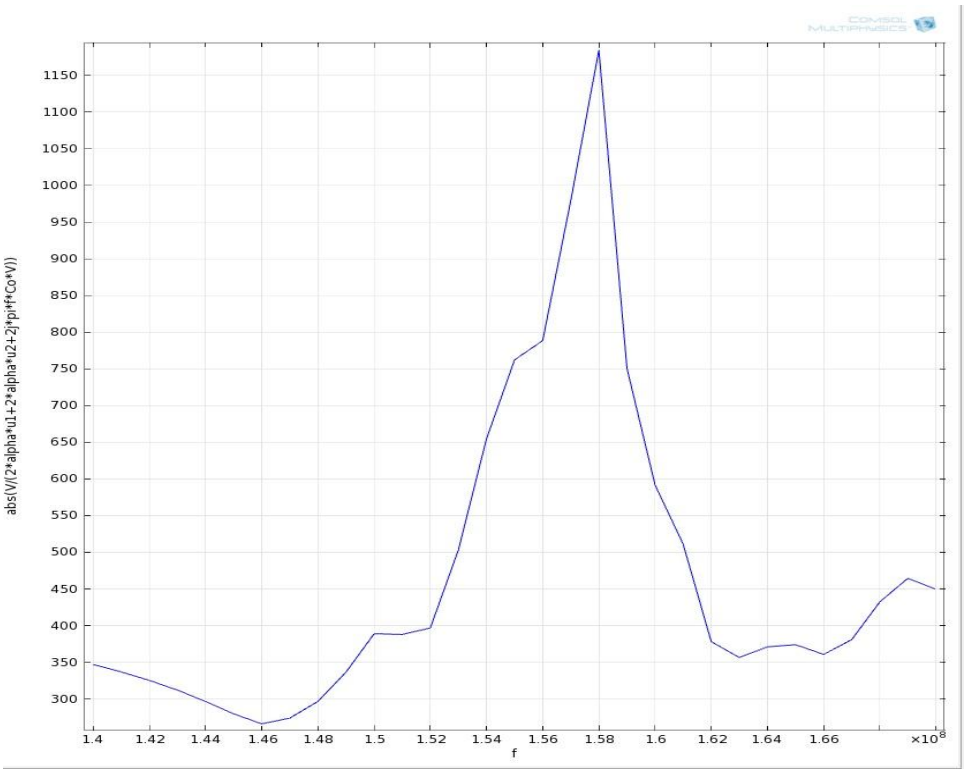

Figure 8: Impedance response curve for modeled SAW device

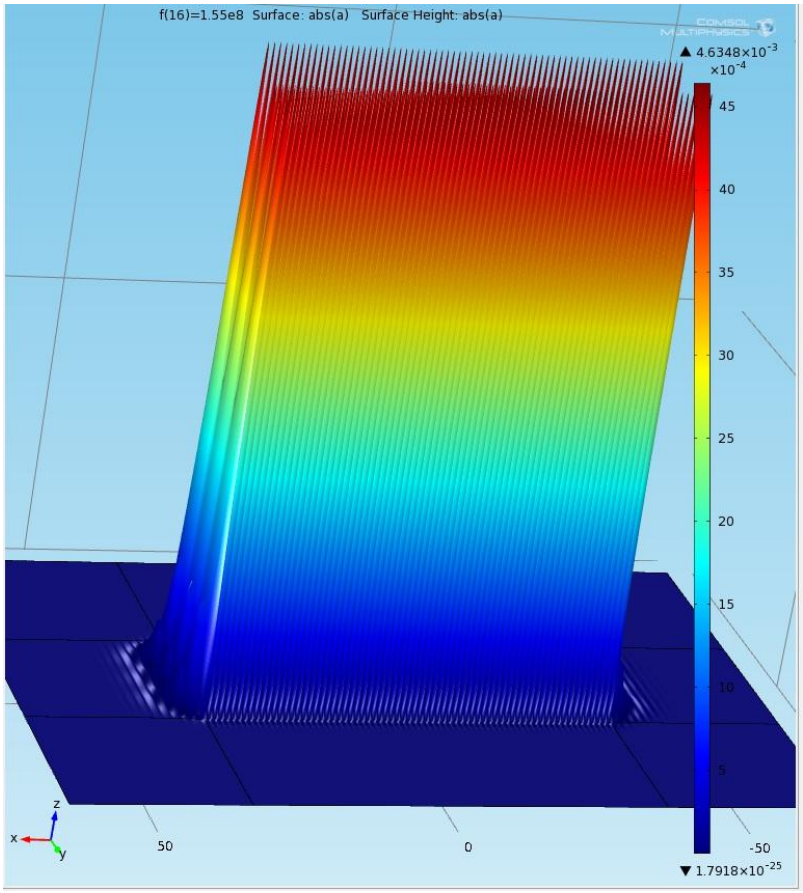

Figure 9: Wave amplitude in solution to modeled SAW device

With the basic 2D model completed, the next goal is to alter the geometry of the device and observe the effects on the impedance response curve.

References

Plesky, Victor and Julius Koskela. "Coupling-of-Modes Analysis of SAW Devices." *International Jounral of High Speed Electronics and Systems* (2000): 867-947.

Schroder, Dieter K. "Surface Voltage and Surface Photovoltage: History, Theory, and Applications." *Measurement Science and Technology* (2001): 16-31.

Tokuda, Osamu and Kazuhiro Hirota. "Two-Dimensional Coupling-of-Modes Analysis in Surface Acoustic Wave Devic e Performed by COMSOL Multiphysics." *Japanese Journal of Applied Physics* (2011): 1-4.

Appendix A1: Additional Figures and Data

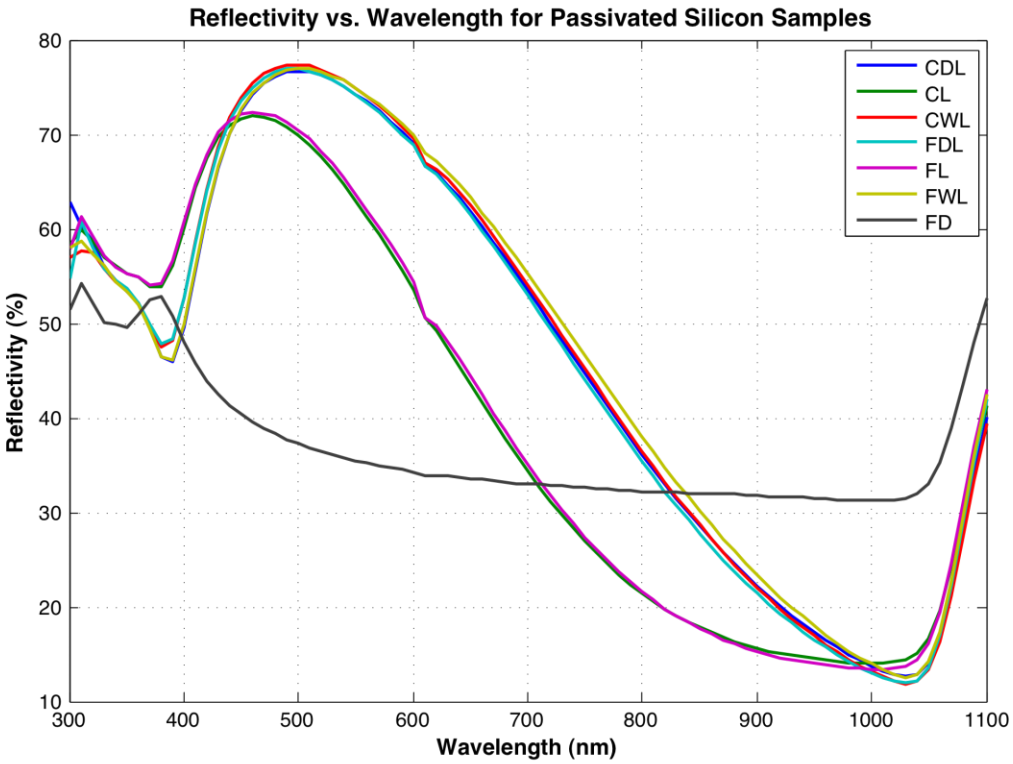

Figure 10: Reflectivities of silicon samples

Sample	Minority Carrier Diffusion Length (cm)	minority carrier lifetime, µs (lower)	minority carrier lifetime, µs (upper)	Surface recombination velocity, cm/s (lower)	Surface recombination velocity, cm/s (upper)
CL	0.0145	4.75	5.20	2789.1	3050.6
CWL	0.0114	2.94	3.21	3547.3	3879.9
CDL	0.0075	1.27	1.39	6344.7	6939.5
FDL	0.0284	17.93	18.24	1590.5	1617.7
FWL	0.0294	19.22	19.54	1453.8	1478.8
FL	0.0087	1.68	1.71	4822.8	4905.5
FD	0.0382	32.44	33.00	1157	1176.8

Figure 11: Parameters for silicon samples determined by SPV measurements

Appendix B: MATLAB Code

Surface Photovoltage Post-Processing:

```
function [Ln, srv_est_avg] = spvdata_Si2()

% function written specifically for passivated silicon samples

global direc;
direc = '\\snl\mesa\Users\cdonnel\Summer2011SPVMeasurements\';

cd([direc 'Text File Outputs']);
fprintf('\n Type "y" or "Y" for yes. \n\n');

%% Constants
T = 293;  %temperature
e = 1.6E-19; %electron charge in coulombs
k = 1.38E-23;  %Boltzmann's constant
ni = 1.5E10; %intrinsic carrier concentration for silicon, cm^-3, at T = 300
K

%% Initialize plots
figure;
ax1 = gca;
hold(ax1,'all');
figure;
ax2 = gca;
hold(ax2,'all');

%% Choose sample type and files to be used (here, file list is hardcoded)
sample = input('Sample Type? (Default Si)  ','s');

if isempty(sample)
    sample = 'Si';
end

if any(strcmpi(sample,{'GaAs';'GaAs/InGaP'}))

    a = textread([direc 'Text File Outputs\GaAs_lambda_vs_alpha_10^-8.txt']);
    lambda = a(:,1)*10^8;
    alpha = a(:,2)*10^8;

else if any(strcmpi(sample,{'Si';'SiP';'Si-P';'SiN';'Si-N'}))
        a = textread([direc 'Text File Outputs\SiAbsorption.txt']);
        lambda = a(:,1);
        alpha = a(:,2);

    end
end
file =
```

```
{'080511a_SiCL';'080511b_SiCWL';'080511a_SiCDL';'080511a_SiFDL';'080511a_SiFW
L';'080511a_SiFL';'080511a_SiFD'};


%%
for N = 1:length(file);

    %%% Open next file and allow user to choose upper and lower wavelength
limit
    %%%
    %%%

    fitlines = 0;

    fprintf(['\n File: ' file{N} '\n']);
    data = textread([direc 'Text File Outputs\' file{N}]);

    [data] = normalize(data,file{N});
    step = data(end,end);

    lowerlim = input(['Lower Limit? >= ' num2str(data(end,1)) ', multiple of
' num2str(step) '  ']);

    if isempty(lowerlim)
        lowerlim = data(end,1);
    end

    upperlim = input(['Upper Limit? <= ' num2str(data(end,2)) ', multiple of
' num2str(step) '  ']);

    if isempty(upperlim)
        upperlim = data(end,2);
    end

    lowerind = find(data(:,1) >= lowerlim,1);
    upperind = find(data(:,1) >= upperlim,1);
    wincludes = data(lowerind:upperind,1); %wavelengths to include
    vincludes = data(lowerind:upperind,2); %photovoltages to include
(normalized for photon flux)

    %%% Interpolate to find best estimate for value of alpha
    %%%
    %%%

    for m = 1:length(wincludes);
        %a_inv(m) = 1/(lininterp(wincludes(m),lambda,alpha));
        a_inv(m) = (84.732/(wincludes(m)*10^-3)-76.417)^-2;
        v_inv(m) = 1/vincludes(m);
        labels(m) = wincludes(m);

    end
```

```
    goodinds = find(a_inv < inf);  %may have gotten some that are in range
below bandgap energy and = 0
    a_inv = a_inv(goodinds);
    v_inv = v_inv(goodinds);
    labels = labels(goodinds);



 %%% Add lines and data labels to plots
    %%%
    %%%

    h = plot(ax1,wincludes,vincludes,'linewidth',2);
    col = get(h,'color');
    g = plot(ax2,a_inv,v_inv,'o','color',col);

    xlim = get(ax2,'XLim');

    for m = 1:length(a_inv)
        t(m) = text(a_inv(m)+.02*(xlim(2) -
xlim(1)),v_inv(m),num2str(labels(m)));
    end

    fitlines(1:length(a_inv),1:3) = [a_inv' v_inv' labels'];


    %%% Give user the opportunity to exclude some data points from the
diffusion length fitline

    if any(fitlines)

        lowerfit = input('Lower Wavelength Limit for Fitline?');
        if isempty(lowerfit)
            lowerfit = min(fitlines(:,3));
        end

        upperfit = input('Upper Wavelength Limit for Fitlines?');
        if isempty(upperfit)
            upperfit = max(fitlines(:,3));
        end

        for m = 1:length(a_inv)
            delete(t(m));
        end

        lowerind = find(fitlines(:,3) >= (lowerfit),1);
        upperind = find(fitlines(:,3) >= (upperfit),1);
        fitlines = fitlines(lowerind:upperind,:);

        set(g,'xdata',fitlines(:,1));
        set(g,'ydata',fitlines(:,2));
```

```
        a = polyfit(fitlines(:,1),fitlines(:,2),1);
        alim = max(fitlines(:,1));
        x = linspace(-1,alim,15000);
        b = polyval(a,x);
        Ln_ind = find(b > 0,1);
        Ln(N) = x(Ln_ind);
        slope(N) = a(1);

        vtest(1:length(fitlines(:,2)),N) = 1./fitlines(:,2);  %building a
matrix of 1/V values that were actually used in the fitline


%plot fitline
        u = plot(ax2,x(find(x>0,1)-5:end),b(find(x>0,1)-5:end),'color',col);

        axes(ax2);

        set(get(get(u,'Annotation'),'LegendInformation'),...
            'IconDisplayStyle','off'); % Exclude line from legend

    end
end


figure;
hold all;


for n = 1:length(file)
    name = file{n};
    if strcmpi(name(11),'C')
        Na = [8E15 8E14];
        mu_n = [1.6E3 1.75E3];

    else if strcmpi(name(11),'F')
            mu_n = [1.75E3 1.78E3];
            Na = [1.5E14 9E13];
        end
    end

    zind = find(vtest(:,n) == 0,1);  %some columns may have zeros since
certain fitlines contain more data than others

    if isempty(zind)  %case that data fills full column
        zind = length(vtest(:,n));
    end

    for p = 1:zind - 1
        for m = 1:2
            no = (ni)^2/(Na(m));
            Dn = (mu_n(m)*k*T)/e;
            srv_est = (vtest(p,n)*e*no*(Ln(n)+a_inv(p)))/(Ln(n)*k*T) -
```

```
(Dn/Ln(n));
            srv_est_avg(n,m) = mean(srv_est);
        end;
    end;

end

leg = {'SiCL';'SiCWL';'SiCDL';'SiFDL';'SiFWL';'SiFL';'SiFD'};
%leg = {'SiCL3';'SiFD3';'SiFDL3';'SiFWL3'};%;'SiFWL';'SiFL';'SiFD'};

    ylabel(ax1,'Voltage(V)','fontweight','bold','fontsize',12);
    xlabel(ax1,'Wavelength(nm)','fontweight','bold','fontsize',12);
    grid(ax1,'on');
    title(ax1,['Wavelength vs. Surface Photovoltage for ' sample '
Samples'],'fontweight','bold','fontsize',12)

legend(ax1,leg);

    ylabel(ax2,'Io(1-R)/Voltage','fontweight','bold','fontsize',12);
    xlabel(ax2,'1/alpha (cm)','fontweight','bold','fontsize',12);
    grid(ax2,'on');
    title(ax2,['1/alpha vs. Io(1-R)/Voltage for ' sample '
Samples'],'fontweight','bold','fontsize',12);
    legend(ax2, leg);


end



%%

function [outdata] = normalize(data,file) %[vincludes] =
filternorm(file,voltages,wavelengths)


        h = 6.626E-34;
        c = 2.998E8;
        area = .5^2*pi;  %cm^2

        %%% Normalizes data for varying light intensities and amplifier gains

        global direc;

        wavelengths = data(:,1);
        outdata = data;


[names,current,freq,filter,inslit,outslit,ligain,sensitivity,tc,ampgain,passb
and,recal,type] = textread([direc 'Excel
Workbooks\SummerSPVFiles.txt'],'%s%f%f%s%f%f%f%f%f%f%s%f%s%*[^\n]');
```

```
        ind = find(strcmp(names,file));
        current = current(ind);
        ligain  = ligain(ind);
        sens = sensitivity(ind)*10^-3;
        ampgain = ampgain(ind);
        filter = filter{ind};

        ind2 = find(strcmp(names,filter));
        filtersens = sensitivity(ind2)*10^-9;

        if recal == 0
            outdata(1:end,1) = outdata(1:end,1) - (900 - 883);
        end

        if ~strcmpi(filter,'none');
            filterdata = textread([direc 'Text File Outputs\' filter]);
%Current vs. wavelength measured from photodiode for the specific filter used
in measurement


else
            filterdata = textread([direc 'Text File Outputs\' NOFILTER
'.txt']); %should always use filter though
        end

        outdata(1:end - 1,2) = .5*sens*data(1:end - 1,2);
        filterdata(1:end - 1,2) = .5*filtersens*filterdata(1:end - 1,2);
        r = textread([direc 'Text File Outputs\Responsivity.txt']);
%responsivity (A/W)
        reflectivity = textread([direc 'Excel
Workbooks\Reflectivity_from_Jose.txt']);
        rheaders = textread([direc 'Excel
Workbooks\ReflectivityHeader.txt'],'%s');

        for n = 1:length(wavelengths) - 1

            fi = lininterp(wavelengths(n),filterdata(:,1),filterdata(:,2));
%measured photocurrent with filter in place
            resp = lininterp(wavelengths(n),r(:,1),r(:,2)); %linear
interpolation to find responsivity
            ind = find(strcmpi(file(11:end),rheaders));

            refl =
.01*lininterp(wavelengths(n),reflectivity(:,1),reflectivity(:,ind+1));
            e = h*c/(wavelengths(n)*10^-9);  %energy per photon
            photon = fi/(resp*e); %photon/sec
            flux = photon/area; %photon/(sec*cm^2)
            outdata(n,2) = data(n,2)/(flux*(1-refl)); %voltage normalized by
photon flux

        end
```

```
    end


%%


    function output = lininterp(val,tabvals,tabdata)

        %%%% Function takes an arbitrary x value (val), and interpolates y
using a list
        %%%% of tabulated x (tabvals) and y (tabdata) values and a linear
interpolation.  If value of x falls below or above tabulated
        %%%% list, output in "NaN"


        ind = find(tabvals >= val,1);


        if isempty(ind) || ind == 1
            output = NaN;
        else


 dval = tabvals(ind) - tabvals(ind - 1);  %width of gap of tabulated x values
in which the input x falls
            dn = tabdata(ind) - tabdata(ind - 1); %width of gap of tabulated
y range
            pct = (val - tabvals(ind - 1))/dval; %percent offset of input x
from lower limit
            output = tabdata(ind - 1) + dn*pct;
        end

    end
```

DISTRIBUTION

1 Christine Donnelly – 15 Central Street, Winchester MA 01890. cdonnelly@stanford.edu (electronic copy)

1	MS0899	RIM-Reports Management	9532 (electronic copy)
1	MS1078	Wahid Hermina	1710 (electronic copy)
1	MS1080	Keith Ortiz	1749 (electronic copy)
1	MS1080	Jose Cruz-Campa	1749 (electronic copy)
1	MS1084	Darren Branch	1714 (electronic copy)
1	MS1085	Michael Cich	1742 (electronic copy)
1	MS1085	Charles Sullivan	1742 (electronic copy)
1	MS1085	Mike Baker	1742 (electronic copy)


Sandia National Laboratories